NONLINEAR ACTIVE NOISE CONTROL FOR INFANT INCUBATORS IN NEO-NATAL INTENSIVE CARE UNITS

Priya Thanigai, Sen M. Kuo and Ravi Yenduri

Department of Electrical Engineering
Northern Illinois University, Dekalb, Illinois 60115

ABSTRACT

Excessive noise in neo-natal care units and inside incubators can have a number of detrimental effects on an infant's health. This paper presents a novel, audio-integrated approach to achieving active noise control (ANC) for infant incubators. This paper also presents the implementation of the robust, nonlinear filtered-X least mean M-estimate algorithm, for reducing impulsive interference in incubators. The healthcare application is further enhanced by integrating the "womb effect", i.e., by using intrauterine and maternal heart sounds, proven to be beneficial to infant health, for masking the residual noise. A computer model for audio-integrated noise cancellation utilizing experimentally measured transfer functions is developed for simulations using real medical equipment noise.

Index Terms – Adaptive noise control, infant incubators, least mean M-estimate algorithm, womb effect, nonlinear adaptive algorithm.

1. INTRODUCTION

This paper explores an innovative healthcare application of ANC systems, a noise-free infant incubator as shown in Figure 1. Control of low-frequency noise has been a source of increasing interest in healthcare, especially for sensitive medical applications like the infant incubator. According to the American Academy of Pediatrics [1], high noise levels are prevalent in neonatal intensive care units (NICU) and thus, in incubators, causing auditory damage to pre-term babies as, their auditory systems are the last to mature.

Figure 1. Infant incubator.

Incubator noise is typically broadband and is generated by equipment such as pumps, fans, and heating machinery. It can be broadly characterized into three types: broadband equipment hum, equipment hum interspersed with high-amplitude random impulses and equipment hum interspersed with low-amplitude periodic impulses. High amplitude impulses (40-50 dB higher than background) are caused mainly due to human activity like banging of metal cabinet doors below the incubator or closing of incubator portholes and low amplitude impulses (10 dB higher than the background) are caused due to machinery that aid in respiration [1]. Figure 2 is an example of real incubator noise in the time domain with segments marked by impulses due to respiratory pumps.

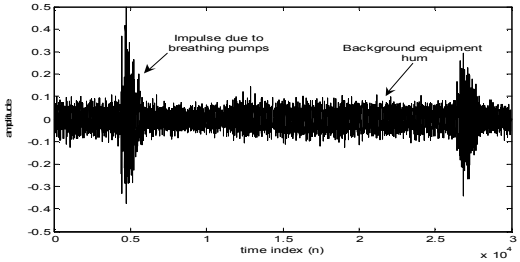

Figure 2. Example waveform of incubator noise.

Section II focuses on developing a conventional ANC system utilizing the filtered-X least mean square (FXLMS) algorithm for cancellation of broadband noise using real transfer functions measured from the laboratory setup. Conventional linear adaptive algorithms however, are not equipped to handle impulsive interference and may exhibit degraded system performance. To enhance algorithm performance in the presence of impulses, the implementation of a nonlinear adaptive algorithm – the filtered-X least mean M-estimate (FXLMM) algorithm is discussed in Section III. This algorithm is capable of handling random and/or periodic impulses and of suppressing the adverse effects of these impulses for incubator ANC application [2].

Section IV outlines the audio-integration algorithm that utilizes the 'womb-effect'. This integration serves two significant purposes – it provides a potential health benefit to infants by utilizing intrauterine sounds, *as heard by the infant* and also masks the residual noise after cancellation.

The algorithm is designed to handle interference from the comfort audio on the performance of the ANC algorithm and ensures that the audio is not canceled by the ANC system. The audio interference cancellation filter also serves as an online secondary path modeling filter.

2. ACTIVE NOISE CONTROL FOR THE INCUBATORS

ANC is based on the principle of utilizing destructive interference to cancel unwanted noise [3]. The FXLMS algorithm is one of the most popular algorithms for ANC. The block diagram of a feedforward broadband ANC system using the FXLMS algorithm is illustrated in Figure 3, where $P(z)$ is the transfer function of the primary path, $S(z)$ is the transfer function of secondary path, and $\hat{S}(z)$ is it's estimate.

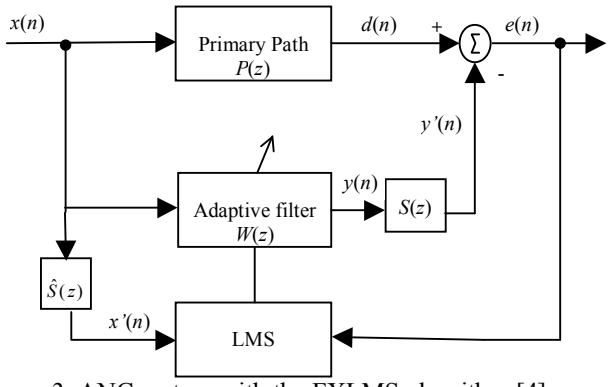

Figure 3. ANC system with the FXLMS algorithm [4].

The ANC system shown in Figure 3 takes into account the effect of the secondary-path by placing an estimate filter in the reference signal path to the least mean square (LMS) algorithm [4]. The experimental setup is as shown in Figure 4, which has the exact dimensions as that of the infant incubator shown in Figure 1. One microphone is placed on both sides of the infant's head. The outputs from both are mixed and analyzed by a spectrum analyzer. The canceling loudspeaker is placed outside the incubator, which can be seen behind the infant's head. The secondary path from the canceling loudspeaker to the error microphones is commonly modeled offline using an adaptive filter with the LMS algorithm.

Figure 4. Experimental setup of incubator.

The offline modeling is done in a unique manner to reduce the annoyance caused due to the usage of white noise. Pleasant natural sounds like that of water are used. Satisfactory results of offline modeling of the secondary path are obtained for a 128-tap adaptive filter and a step size of 0.09, and are shown in Figure 5. The solid line represents the actual transfer function whereas the dotted line represents the estimated one. As is seen, the two lines indicate that the modeling is very close.

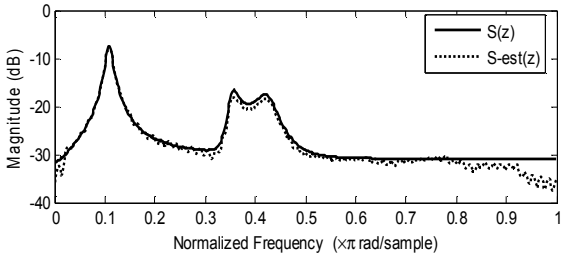

Figure 5. Magnitude responses of the original and the estimated secondary paths.

The input reference noise is taken from an incubator noise audio file. The ANC system shown in Figure 3 is simulated with measured $P(z)$ and $S(z)$. A 256-tap filter and a step size of 0.06 are used for the adaptive noise cancellation filter $W(z)$. The residual noise is found to be 16 dB lower than the input on average. The plot illustrating the spectra of noise before (ANC OFF) and after (ANC ON) cancellation is shown in Figure 6. The next section discusses the implementation of nonlinear FXLMM algorithm for suppressing impulse noise.

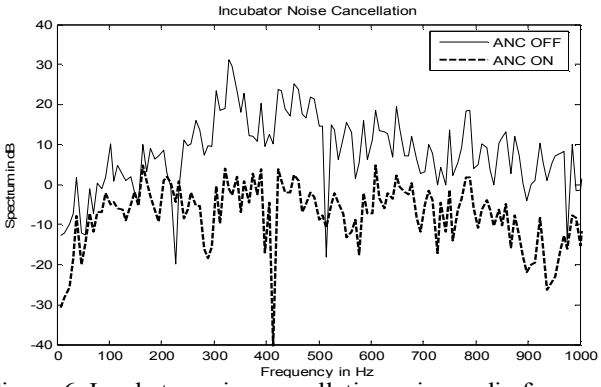

Figure 6. Incubator noise cancellation using audio for offline modeling.

3. NONLINEAR ALGORITHM FOR IMPULSE NOISE SUPRESSION

The performance of linear adaptive filters can degrade significantly in the presence of impulse noise, thus nonlinear algorithms are preferred to reduce the adverse effects [7]. The FXLMM algorithm is a simple and robust method that employs the mean M-estimate error objective function [2] [5] and is capable of performing effectively in impulsive

environments. Consider Figure 3, the residual signal is given as,

$$e(n) = d(n) - s(n) * [\mathbf{w}^T(n)\mathbf{x}(n)] \quad (1)$$

where $\mathbf{w}(n) = [w_0(n)\ w_1(n)\ \ \dots\ \ w_{N-1}(n)]^T$ is the coefficient vector of adaptive filter $W(z)$ at time n, $\mathbf{x}(n) = [x(n)\ \ x(n\text{-}1)\ \dots\ \ x(n\text{-}N\text{+}1)]^T$ is the reference signal vector at time n, $s(n)$ is the impulse response of the secondary-path $S(z)$, and * denotes linear convolution [4].

The objective of the adaptive filter $W(z)$ is to minimize the weighted least M-estimate function criterion $\xi(n) = \sum_{i=1}^{n} \lambda^{n-i} \rho[e(i)]$ where $\rho(.)$ is the M-estimate function. The weight vector $\mathbf{w}(n)$ is updated in the negative direction of the gradient vector

$$\mathbf{w}(n+1) = \mathbf{w}(n) - \mu \nabla J_{M\rho} \quad (2)$$

where the objective function for the adaptive filter is as given [2]

$$J_{M\rho} \equiv E[\rho[e(n)]] \cong \rho[e(n)] \quad (3)$$

This function is minimized by updating the weight vector in a negative direction of the gradient vector given by

$$\nabla J_{M\rho} = \frac{\partial J_{M\rho}(n)}{\partial \mathbf{w}(n)} = \frac{\partial \rho[e(n)]}{\partial e(n)} \frac{\partial e(n)}{\partial \mathbf{w}(n)} \quad (4)$$

Let $\psi[e(n)]$ be the first order partial derivative of $\rho[e(n)]$, the gradient now becomes

$$\begin{aligned} \nabla J_{M\rho} &= \psi[e(n)] \frac{\partial e(n)}{\partial \mathbf{w}(n)} \\ &= \psi[e(n)][-s(n) * \mathbf{x}(n)] \\ &= -q[e(n)]e(n)[s(n) * x(n)] \end{aligned} \quad (5)$$

where the weight vector $q[e(n)] \equiv \psi[e(n)]/e(n)$. Since $s(n)$ is the impulse response of the secondary-path, which is not available directly, an estimate of the secondary-path $\hat{S}(z)$ is modeled and its impulse response $\hat{s}(n)$ is used.

Substituting the estimate in equation (5) we get

$$\begin{aligned} \nabla J_{M\rho} &\cong -q[e(n)]e(n)[\hat{s}(n) * \mathbf{x}(n)] \\ &= -q[e(n)]e(n)x'(n) \end{aligned} \quad (6)$$

Substituting equation (6) into equation (1) we get the weight vector update equation for the FXLMM algorithm as,

$$\mathbf{w}(n+1) = \mathbf{w}(n) + \mu q[e(n)]e(n)\mathbf{x}'(n) \quad (7)$$

The function $\rho(.)$ is chosen as the Hampel's three-part redescending M-estimate function [2], which is known for its computational simplicity. It is defined as

$$\rho[e(n)] = \begin{cases} e^2(n)/2, & 0 \le |e(n)| < \xi \\ \xi|e(n)| - \xi^2/2, & \xi \le |e(n)| < \Delta_1 \\ \xi/2(\Delta_1 + \Delta_2) - \xi^2/2 + [\xi|e(n)| - \Delta_2)^2]/2(\Delta_1 - \Delta_2), & \Delta_1 \le |e(n)| < \Delta_2 \\ \xi/2(\Delta_1 + \Delta_2) - \xi^2/2, & \Delta_2 \le |e(n)| \end{cases} \quad (8)$$

The simulation results using the FXLMM algorithm with comparative case studies from the FXLMS algorithm are detailed in the following section. The FXLMM algorithm was implemented for incubator noise interspersed with high-amplitude random impulses (30 dB higher than background). The impulses are at time n = 40000, 52000 and 64000 and last for a length of 100 samples. The probabilities θ_ξ, $\theta_{\Delta 1}$, and $\theta_{\Delta 2}$ for determining the threshold were taken to be 0.05, 0.025 and 0.01, respectively, for 95%, 97.5% and 99.5% confidence that the error vector was in the interval $[\xi\ \Delta_1]$, $[\Delta_1\ \Delta_2]$ and $e(n) > \Delta_2$, respectively [2]. A 256-tap adaptive filter was implemented for a step size of 0.06. The learning curves for the FXLMS and FXLMM algorithms are shown in Figure 7.

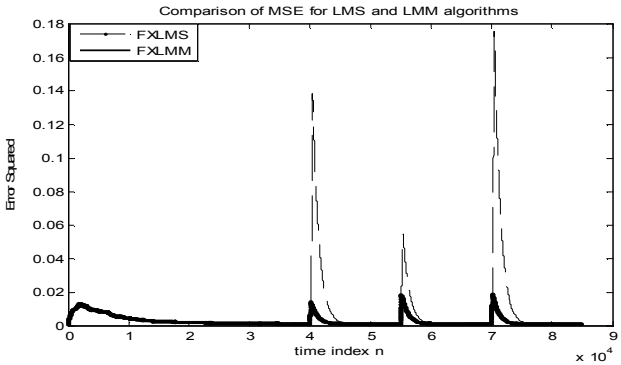

Figure 7. Learning curves for $\mu_{FXLMS} = \mu_{FXLMM} = 0.06$. Impulse occurred at n = 40000, 52000 and 64000.

The simulation shows that the FXLMM algorithm behaves in an identical manner to the FXLMS algorithm until before the impulses are encountered. The FXLMS algorithm, however, exhibits degraded system performance with a very high mean squared error (MSE) in the presence of impulses. The FXLMM algorithm is found to be more robust while handling impulses. Comparing the MSE plots of the two algorithms shows that the FXLMM algorithm has superior performance in the presence of impulses and is more effective in suppressing the adverse influence of impulse noise.

4. INTEGRATED ANC SYSTEM WITH "WOMB" AUDIO

This section focuses on developing an algorithm that can integrate "comfort" audio with the existing ANC system to provide an environment conducive to good infant health and to mask the undesired residual noise. The comfort audio used is a combination of maternal heartbeat and other intrauterine sounds [8]. Research has proven that playing womb sounds showed significant differences in the respiration rate, sleep cycle, and oxygen saturation in infants [6]. Unfortunately, the audio signal that is added to the output of the ANC filter, however, can act as interference to any ANC algorithm. Hence, a method must be devised to subtract the audio from the error signal before it is used to update the coefficients of the adaptive filter. In Figure 8, an adaptation of Figure 3, the comfort audio $a(n)$ is added to the antinoise $y(n)$ that can be heard by the infant inside the incubator.

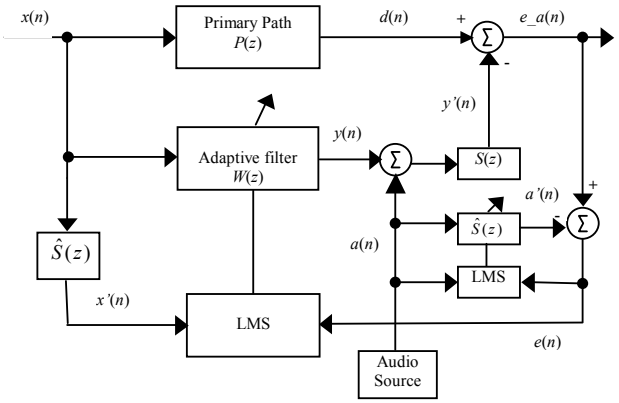

Figure 8. Block diagram of audio-integrated ANC system.

At the acoustic summing junction, $y'(n)$ and $d(n)$ are combined to produce residual error $e\_a(n)$. The audio component is subtracted from this error to provide the "true" error $e(n)$. It should be noted that the audio is filtered through $S(z)$ before it is subtracted. The error $e\_a(n)$ is expressed in the z-domain as:

$$\mathbf{E}\_\mathbf{A}(z) = \mathbf{D}(z)\mathbf{S}(z)\left[\mathbf{Y}(z) + \mathbf{A}(z)\right] \tag{9}$$

The adaptive filter $\hat{S}(z)$ is used to cancel the audio interference on the performance of $W(z)$. This filter generates

$$\mathbf{E}(z) = \mathbf{E}\_\mathbf{A}(z) + \mathbf{S}(z)\mathbf{A}(z) \tag{10}$$

Substituting equation (9) into (10) we get

$$\mathbf{E}(z) = \mathbf{D}(z)\mathbf{S}(z)\mathbf{Y}(z) \tag{11}$$

This is the "true" error which is used to update the adaptive filter $W(z)$.

The main advantage of this algorithm lies in its ability to model the secondary-path online. Online modeling of the secondary path involves its estimation in tandem with the operation of the ANC system. The filter is modeled through an adaptive system identification scheme that uses comfort audio as the reference signal and treats the secondary path as the unknown system.

A simulation model of Figure 8 is set up for a 256-tap adaptive filter $W(z)$ with a step size of 0.06 as before. The secondary path is estimated using a 128-tap filter and a step size of 0.095. The ANC system is allowed to converge, and the error signal reaches a steady state before the audio is added. Figure 9 illustrates that the audio integration algorithm allowed proper convergence of the adaptive filter.

We can summarize the advantages of the audio integrated ANC system as follows: (i) it provides a pre-natal ambience, thus nurturing the health of the infant. (ii) it is successful in masking residual error and in preventing the audio from interfering with the algorithm updation. (iii) the secondary path is modeled online, making the system more responsive to changes in the environment. (iv) the audio integration does not require additional hardware, existing speakers and power amplifier of the ANC system can be used making it cost-effective.

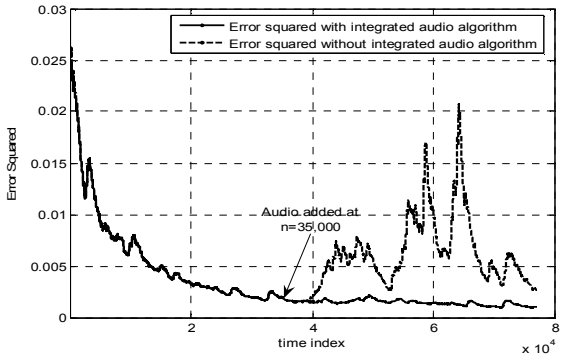

Figure 9. Learning curves with and without the integrated audio algorithm.

5. CONCLUSIONS

In this paper, an innovative application of ANC systems, the infant incubator was presented. Real transfer functions from a laboratory setup were used to develop a computer model for simulation. Simulation results showed an average cancellation of 16 dB. This paper also presented the development and implementation of the robust, nonlinear FXLMM algorithm for reducing impulsive interference. The function of the ANC system was further enhanced by using an algorithm that integrated comfort audio and modeled the secondary path online. The comfort audio provided a beneficial environment for the infant's growth and masked the residual noise from the ANC system.

REFERENCES

[1] Quest Technology, "Noise in Neonatal Intensive Care Units," User Application Note 3, 2002.

[2] Y. Zou, S. C. Chan and T. S. Ng, "Least Mean M-Estimate Algorithms for Robust Adaptive Filtering in Impulse Noise," *IEEE Trans. on Circuits and Systems II*, vol. 47, pp. 1564-1569, 1999.

[3] S. J. Elliot and P. A. Nelson, "Active Noise Control," *IEEE Signal Processing Magazine*, vol. 10, pp. 12-35, October 1993.

[4] S. M. Kuo and D. R. Morgan, *Active Noise Control Systems Algorithms and DSP Implementations*, New York: Wiley, 1996.

[5] Y. Zou, S. C. Chan and T. S. Ng, "A Robust M-estimate Adaptive Filter for Impulse Noise Suppression," *International Conference on Acoustics, Signal and Speech Processing*, vol. 4, pp. 1765-1768, May 1999.

[6] J. M. Standley, "A Meta-Analysis of the Efficacy of Music Therapy for Premature Infants," *Journal of Pediatric Nursing*, vol. 17, no. 2, pp. 107 – 112, April 2002.

[7] P. J. Rousseeuw and A. M. Leroy, *Robust Regression and Outlier Detection*, Wiley & Sons, New York, 1987.

[8] Babysleep System®, from http://www.babysleepsystem.com/babysleep/system.htm